

MULTI-SPATIAL SCALE AEROSOL OPTICAL THICKNESS MAPPING FOR BEIJING USING REMOTE SENSING TECHNIQUE

Jie Guang^{a,b}, Yong Xue^{a,c*}, Xiaowen Li^a, Linyan Bai^{a,b}, Ying Wang^{a,b}, Yingjie Li^{a,b}, Wei Wan^{a,b}, Jianping Guo^d

^a State Key Laboratory of Remote Sensing Science, Jointly Sponsored by the Institute of Remote Sensing Applications of Chinese Academy of Sciences and Beijing Normal University, Institute of Remote Sensing Applications, Chinese Academy of Sciences, Beijing 100101, China

^b Graduate School of the Chinese Academy of Sciences, Beijing 100039, China

^c Department of Computing, London Metropolitan University, 166-220 Holloway Road, London N7 8DB, UK

^d Center for Atmosphere Watch and Services, Chinese Academy of Meteorological Sciences, Beijing 100081, China
-guangjier@163.com, yxue@irsa.ac.cn

Commission VIII, WG VIII/3

KEY WORDS: Multi-spectral remote sensing; Scale; Image understanding; Spatial modelling; Environmental monitoring; Urban; Multi-sensor

ABSTRACT:

Aerosol particles play an important role in many atmospheric processes and affect global energy budget since they absorb and scatter solar radiation. In addition, aerosol particles take part in many heterogeneous chemical reactions and have adverse effects on human health. Retrieval of aerosol optical thickness (AOT) over bright land is still a challenging and imperative problem due to the complexity added by the variability of the land surface characteristics. In this paper, multi-spatial scale aerosol optical thickness mapping for Beijing was made using MODIS and ASTER data. The spatial resolution of aerosol optical thickness products are 15m, 250m, 500m, 1km and 10km, respectively. To retrieve AOT from MODIS data, the synergy of Terra and Aqua MODIS data algorithm and BRDF models were used. The BRDF characteristics of ground surfaces are considered by combining the geometrical information of solar and sensors extracted from MODIS data and linear kernel-driven BRDF parameter products (MOD43). An operation bi-angle approach was used to retrieve AOT from ASTER data. Validation is performed by comparison with AERONET (Aerosol Robotic Network) ground-based Sun-photometer data and the MODIS aerosol products (MOD04). Results show that the primary trend of AOT distribution for different spatial scales over the same region is consistent. When zoom in to details, the distribution of AOT are different between multi-spatial scales.

1. INTRODUCTION

Aerosols are one of the greatest sources of uncertainty in climate modelling, which play a significant role in the Earth's radiation budget through radiative forcing and chemical perturbations (Kaufman et al., 2002a). In addition, epidemiological studies showed that respiratory symptoms, lung function and mortality are significantly correlated with the mass density of the particulate matter below $10\mu\text{m}$ (Stedman, 2004). Hence it is desirable to obtain information on aerosol properties both globally as well as on a local or regional scale. Due to their high temporal and spatial variability, atmospheric aerosol monitoring presents a difficult task, and thus significant efforts have been made to improve aerosol characterization by using in situ measurements (Anderson et al., 2003), ground-based remote sensing (Holben et al., 2001), satellite observations (Kaufman et al., 2002b), and aerosol transport modelling (Chin et al., 2002). Utilization of satellite observations in the visible and near-IR over arid or unvegetated surfaces presents a more challenging task because the satellite signal is dominated by a large surface contribution (Kaufman et al., 1997).

The approach of the present study is to combine satellite observations with collocated ground-based measurements to retrieve AOT over bright land. Multi-spatial scale aerosol

optical thickness mapping for Beijing was made using MODIS and ASTER data. In order to evaluate the impact of spatial resolution, we provide comparisons of validated 15m AOT from ASTER data to those derived from the 250m, 500m, and 1km resolutions of MODIS data and the 10km MODIS aerosol products (MOD04).

2. DATA SETS

Two data sets of the Moderate Resolution Imaging Spectroradiometer (MODIS) and the Advanced Spaceborne Thermal Emission and Reflection Radiometer (ASTER) were selected for the study of multi-spatial scale aerosol distribution. As MODIS and ASTER onboard the same satellite (EOS Terra), the temporal differences between them can be ignored.

MODIS onboard NASA's Terra and Aqua satellites performs single view angle observations in a wide spectral range providing images in 36 spectral bands with spatial resolution 250m, 500m and 1km. The MODIS Aerosol Product monitors the ambient aerosol optical thickness over the oceans globally and over a portion of the continents. Daily Level 2 data are produced at the spatial resolution of a 10km. MODIS/Terra+

* Corresponding author

Aqua BRDF/Albedo Model Parameters are operationally produced every 16 days at a 1km (MCD43B1) and a 500m (MCD43A1) spatial resolution. The MODIS data are obtained from <http://ladswb.nascom.nasa.gov>.

ASTER is an advanced multi-spectral imager that was launched onboard NASA's Terra spacecraft in December 1999. ASTER covers a wide spectral region with 14 bands from visible to thermal infrared with high spatial, spectral and radiometric resolutions. An additional 27.6° backward-looking near-infrared band provides stereo coverage. The spatial resolution varies with wavelength: 15m in the visible and near-infrared (VNIR), 30m in the short wave infrared (SWIR), and 90m in the thermal infrared (TIR).

AERONET is a federation of ground-based remote sensing instruments measuring aerosol and its characteristics. The network imposes standardization of instruments, calibration and processing. The level 1.0 product is used in this study and the accuracy of the AERONET aerosol optical depth measurements is ~0.01 for the wavelength ≥ 0.44μm (Eck et al., 1999).

3. RETRIEVAL METHODS

3.1 AOT retrieval from 1km and 500m MODIS data

Terra MODIS and Aqua MODIS are viewing the entire Earth's surface every 1 to 2 days. The interval of the two satellites pass over the same area is usually less than 3 hours. These data will improve our understanding of the aerosol characteristics. A new method based on SYNTAM algorithm (Tang et al., 2005) is proposed to retrieval AOT from MODIS data. Improvement of this approach was made in using the BRDF (bi-directional reflectance distribution function) models to consider the ground surface bi-directional property.

The aerosol retrieval model bases on Equation (1).

$$R_{j,\lambda_i} = \frac{(R'_{j,\lambda_i} b - a_j) + a_j(1 - R'_{j,\lambda_i})e^{(a_j-b)\epsilon\tau_0^{\lambda_i} \sec\theta'_j}}{(R'_{j,\lambda_i} b - a_j) + b(1 - R'_{j,\lambda_i})e^{(a_j-b)\epsilon\tau_0^{\lambda_i} \sec\theta'_j}} \quad (1)$$

where $j=1,2$, respectively stand for the observation of TERRA-MODIS and AQUA-MODIS; $i=1,2,3,\dots$ stand for MODIS bands; λ is the central wavelength. R is the Earth's surface reflectance. R' is the Earth's system reflectance (top of atmospheric reflectance); $a=\sec\theta$ and $b=2$, ϵ is the backscattering coefficient, typically 0.1. θ is the solar zenith angle, θ' is the sensor zenith angle.

Two assumptions were made, that are a horizontally-stratified atmosphere and considering no aerosol and water vapour spectral absorbing effect. Our method only takes account of the scattering of atmospheric molecular and aerosol particles. For the molecular Rayleigh scattering, Linke (1956) has given an approximate expression, which is sufficiently accurate for most application in remote sensing:

$$\tau_0^\lambda = \tau_M^\lambda(\infty) + \tau_A^\lambda(\infty) \quad (2)$$

$$\tau_M^\lambda(\infty) = 0.00879\lambda^{-4.09} \quad (3)$$

According to the Angstrom's turbidity equation:

$$\tau_A^\lambda(\infty) = \beta\lambda^{-\alpha} \quad (4)$$

Now, if we substitute bi-temporal satellite data such as three visible spectral bands data, central wavelength of 0.47, 0.55, 0.66μm, respectively, from TERRA and AQUA into Equation (1), we can obtain one group of nonlinear equations as follows:

$$A_{j,\lambda_i} = \frac{(A'_{j,\lambda_i} b - a_j) + a_j(1 - A'_{j,\lambda_i})e^{(a_j-b)\epsilon(0.00879\lambda_i^{-4.09} + \beta_j\lambda_i^{-\alpha}) \sec\theta'_j}}{(A'_{j,\lambda_i} b - a_j) + b(1 - A'_{j,\lambda_i})e^{(a_j-b)\epsilon(0.00879\lambda_i^{-4.09} + \beta_j\lambda_i^{-\alpha}) \sec\theta'_j}} \quad (5)$$

The bidirectional reflectance properties of the ground surface depend not only on the wavelength but also on the geometry. The operational MODIS BRDF/Albedo algorithm makes use of a kernel-driven, linear BRDF model which relies on the weighted sum of an isotropic parameter and two functions (or kernels) of viewing and illumination geometry to determine reflectance, R (Schaaf, 2002).

$$R(\theta_s, \theta_v, \phi, \lambda_i) = f_{iso}(\lambda_i) + f_{vol}(\lambda_i)K_{vol}(\theta_s, \theta_v, \phi) + f_{geo}(\lambda_i)K_{geo}(\theta_s, \theta_v, \phi) \quad (6)$$

where θ_s , θ_v , and ϕ are the solar zenith, view zenith and relative azimuth angles; $K_k(\theta_s, \theta_v, \phi)$ are the model kernels; $f_k(\lambda)$ are the spectrally dependent BRDF kernel weights or parameters. The kernel weights selected are those that best fit the available observational data. One of these kernels, $K_{vol}(\theta_s, \theta_v, \phi)$ is derived from volume scattering radiative transfer models (Ross, 1981) and the other, $K_{geo}(\theta_s, \theta_v, \phi)$ from surface scattering and geometric shadow casting theory (Li & Strahler, 1992).

With the solar and sensor zenith and azimuth angles captured from MOD021KM (Level 1B calibrated relocated radiances) and BRDF model parameters from MCD43B1 (1km spatial resolution) or MCD43A1 (500m spatial resolution), we can reconstruct ground surface reflectance of Band 1~7 of Terra and Aqua. The ratio of two views' surface reflectance can be written as follows:

$$K_{\lambda_i} = \frac{R_{Terra,\lambda_i}}{R_{Aqua,\lambda_i}} \quad (7)$$

Combined with equation (7), the equation (5) can be solved by means of Newton iteration algorithm, accounting for the difficulty in getting analytical solution. We can obtain the aerosol parameters α (wavelength exponent) and β (Angstrom's turbidity coefficient) simultaneous with surface reflectance R .

3.2 AOT retrieval from 250m MODIS data

There are only two bands have 250m spatial resolution, so we use the α (wavelength exponent) as the known number input the equation (5), then the unwieldy problem can be solved and we can get the AOT and surface reflectance of band 1 and band 2 with 250m spatial resolution.

3.3 AOT retrieval from ASTER data

Similar to the bi-angle approach describe above in 3.1, we developed the ASTER AOT retrieval model exploiting the dual-angle view capability of ASTER (Guang et al., 2008).

4. RESULTS AND ANALYSIS

We applied the retrieval methods to joint sets of ground-based Beijing AERONET data and satellite observations (MODIS and ASTER data) over Beijing, China on April 9th, 2004, which day a substantial aerosol load was observed on the basis of sun photometer records and ground level PM10 measurements. The original images are shown in Figure 1 and Figure 2. ASTER image scope is part of the scope of MODIS image.

4.1 Validation

The retrieval results are compared to the result of ground-based aerosol measurements by a sun photometer at the AERONET Beijing site for validation, which are shown in Table 1. AERONET GMT Time is 03:16, and Terra/MODIS pass time is 03:10. The wavelengths measured by AERONET include 0.44-, 0.675-, 0.87- and 1.02 μm , therefore, in order to compare with AOT retrieved from MODIS and ASTER, the AERONET optical thickness has to be determined for the equivalent wavelength as MODIS and ASTER by Angstrom's turbidity equation. The validation of the retrieval AOT shows that the results are consistent with AERONET AOT.

Wave length (μm)	AERO NET	Terra/MODIS (1km)	Terra/MODIS (500m)	Terra/MODIS (250m)	ASTER
0.47	0.574	0.551	0.595	—	—
0.55	0.496	0.470	0.512	—	—
0.66	0.419	0.403	0.443	0.407	—
0.807	0.348	—	—	—	0.350
0.86	0.328	—	—	0.320	—

Table 1. AOT comparison between the satellite retrieval results and Level 1.0 data from AERONET

4.2 Comparison between 250m MODIS AOT and 15m ASTER AOT

When zoom in to details, the distribution of AOT are different between 250m MODIS AOT and 15m ASTER AOT. Figure 3 and Figure 4 shows that difference. Most differences are within ± 0.1 . Possible origin of these differences is the changes in TOA (Top of atmosphere) reflectance at different spatial resolutions.

4.3 Comparison between MODIS AOT retrievals

The AOT derived from the 250m, 500m, and 1km resolutions of Terra/MODIS data at $\lambda=0.55\mu\text{m}$ are shown in Figure 5a, Figure 5b and Figure 5c, respectively. Figure 6 is AOT at $\lambda=0.55\mu\text{m}$ from MODIS aerosol products MOD04_L2.

To investigate the effect of changes in resolution on MODIS AOT retrievals, statistical analysis of the retrieved AOT at resolution of 250m, 500m, 1km and 10km are shown in Table 2.

Variable	250m AOT	500m AOT	1km AOT	10km AOT
Mean	1.409	0.794	0.828	0.358
Standard Deviation	4.816	0.496	0.478	2.296

Table 2. Statistical value of the retrieved AOT at resolution of 250m, 500m, 1km and 10km

In general, the primary trend of AOT distribution of MODIS is consistent over the same region. The AOT results retrieved from 250m, 500m, 1km have good consistence, and 250m AOT result shows more details than others as the standard deviation is the largest. 10km AOT from MOD04_L2 are lower than the 1km retrieved AOT except in the south-east of Beijing.

5. CONCLUSIONS AND DISCUSSION

In this paper, aerosol optical thickness at 4 different spatial resolutions (15m, 250m, 500m and 1km) were retrieved using MODIS and ASTER data. Preliminary results indicated that multi-spatial scale of data is successfully combined to retrieve AOT, especially for the bright surface such as urban city which can't get from MODIS aerosol products in MOD04_L2. Compared with the AERONET aerosol products, the retrieval results are acceptable but it is also require more verification. Uncertainties of our method are mainly introduced by factors such as aerosol and water vapour spectral absorption, registration of two temporal images, sub-pixel cloud contamination, and our assumptions on invariant α , which should be taken into account in future research. The multi-spatial scale aerosol optical thickness mapping of Beijing provided aerosol distribution in different scales, which can be used as the prior knowledge for retrieving AOT with multi-source data in future.

REFERENCES

- Anderson, T. L.; Masonis, S. J.; Covert, D. S.; Ahlquist, N. C.; Howell, S. G.; Clarke, A. D., et al. 2003. Variability of aerosol optical properties derived from in situ aircraft measurements during ACE-Asia. *Journal of Geophysical Research*, 108, 8647. doi:10.1029/2002JD003247.
- Chin, M.; Ginoux, P.; Kinne, S.; Torres, O.; Holben, B. N.; Duncan, B. N., et al. 2002. Tropospheric aerosol optical thickness from the GOCART model and comparisons with satellite and Sun photometer measurements. *Journal of the Atmospheric Sciences*, 59, pp. 461-483.
- Eck, T. F.; Holben, B. N.; Reid, J. S.; Dubovik, O.; Smirnov, A.; O'Neill, N. T., et al. 1999. Wavelength dependence of the optical depth of biomass burning, urban, and desert dust aerosols. *Journal of Geophysical Research*, 104, pp. 31333-31349.
- Guang, J.; Xue Y.; Bai L.Y.; Guo J.P., 2008. Application of AOT products derived from ASTER data to the air pollution research around the Beijing Olympic Games area. In: *Proceedings of SPIE-Remote Sensing of the Environment: 16th National Symposium on Remote Sensing of China, 2007*.(in press)

Holben, B. N.; Tanre, D.; Smirnov, A.; Eck, T. F.; Slutsker, I.; Abuhassan, N., et al. 2001. An emerging ground-based aerosol climatology: Aerosol optical depth from AERONET. *Journal of Geophysical Research*, 106, pp. 12067-12097.

Kaufman, Y. J.; Tanré, D.; & Boucher, O. 2002a. A satellite view of aerosols in the climate system. *Nature*, 419, pp. 215-223.

Kaufman, Y. J.; Gobron, N.; Pinty, B.; Wildowski, J. L., & Verstraete, M. M. 2002b. Relationship between surface reflectance in the visible and midinfrared used in MODIS aerosol algorithm: Theory. *Geophysical Research Letters*, 29. doi:10.1029/2003JD003981.

Kaufman, Y. J.; Tanre, D.; Remer, L. A.; Vermote, E. F.; Chu, A.; & Holben, B. N. 1997. Operational remote sensing of tropospheric aerosol over land from EOS moderate resolution imaging spectroradiometer. *Journal of Geophysical Research*, 102, pp. 17051-17068.

Li, X., & Strahler, A. H., 1992. Geometric-optical bidirectional reflectance modeling of the discrete crown vegetation canopy: effect of crown shape and mutual shadowing. *IEEE Trans. Geosci. Remote Sens.*, 30, pp. 276-292.

Ross, J. K., 1981. *The radiation regime and architecture of plant stands*. Norwell, MA: Dr. W. Junk, pp. 392.

Schaaf C. B.; Gao F.; Strahler A. H., et al., 2002. First operational BRDF albedo nadir reflectance products from MODIS. *Remote Sensing of Environment*, 83, pp. 135-148.

Stedman, J. R., 2004. The predicted number of air pollution related deaths in the UK during the August 2003 heatwave. *Atmospheric Environment*, 38(8), pp. 1087-1090.

Tang J. K.; Xue Y.; Yu T.; Guan Y. N., 2005, Aerosol Optical Thickness Determination by Exploiting the Synergy of TERRA and AQUA MODIS (SYNTAM). *Remote Sensing of Environment*, 94(3), pp. 327-334.

ACKNOWLEDGEMENTS

This work is an output from the research projects funded by NSFC under Grant Nos. 40471091 and 40671142, "973 Project -Active and passive remote sensing of land surface ecological and environmental parameters" (2007CB714402) by MOST, China and "Multi-sources quantitative remote sensing retrieval and fusion" (KZCX2-YW-313). The authors thank EOS Gateway and LPDAAC for the MODIS data. Many thanks go to the PI investigators of Beijing AERONET site used in this paper.

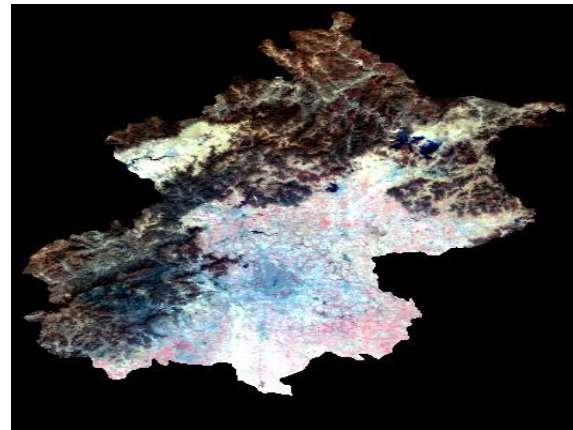


Figure 1. Terra/MODIS reflectance RGB (R for Band 2; G for Band 1; B for Band 4) composed image (500m spatial resolution)

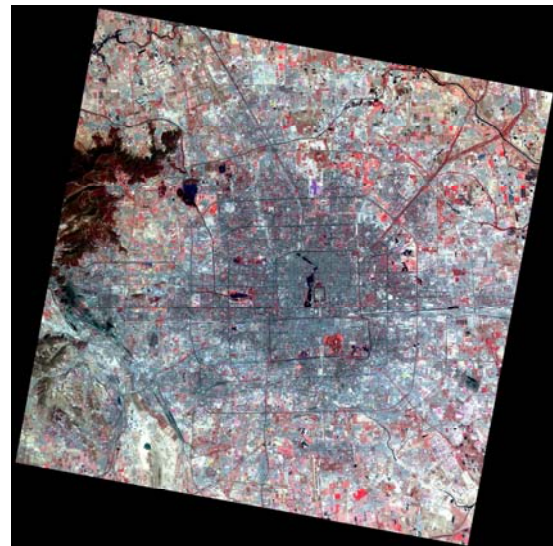


Figure 2. ASTER reflectance RGB (R for Band 3; G for Band 2; B for Band 1) composed image

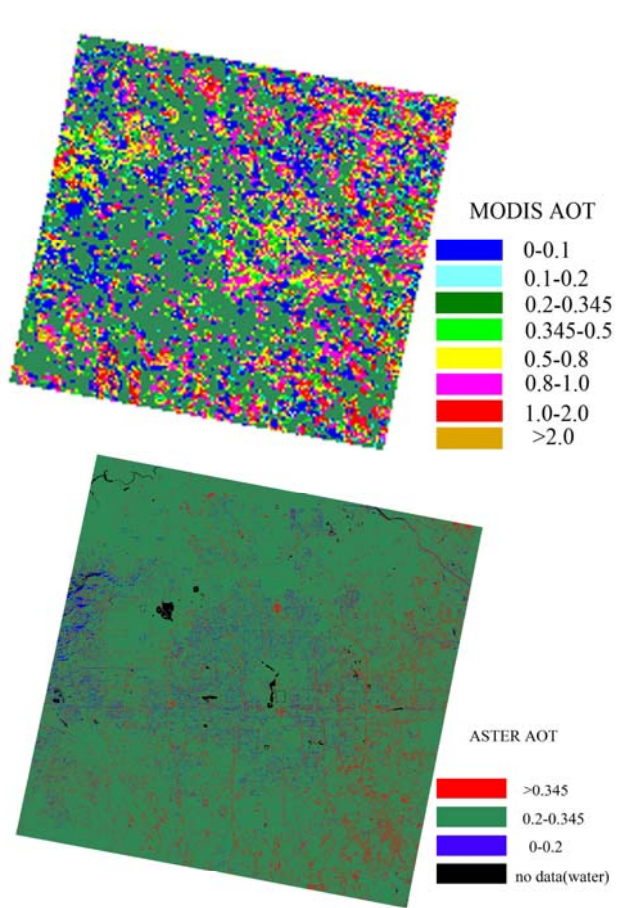


Figure 3. Contrast between the AOT retrieved for the 250m Terra/MODIS band 2(0.86 μ m) and ASTER band 3N (0.807 μ m)

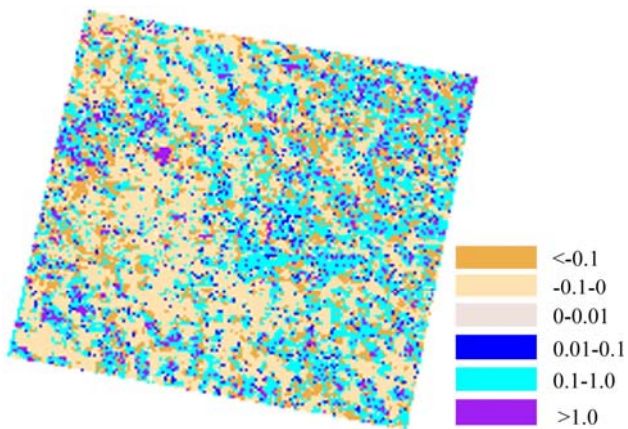


Figure 4. Difference of AOT retrieved for the Terra/MODIS band 2 and ASTER band 3N. Blue colour represents AOT value retrieved from MODIS is larger than that of ASTER DATA. The other colour represents the contrary.

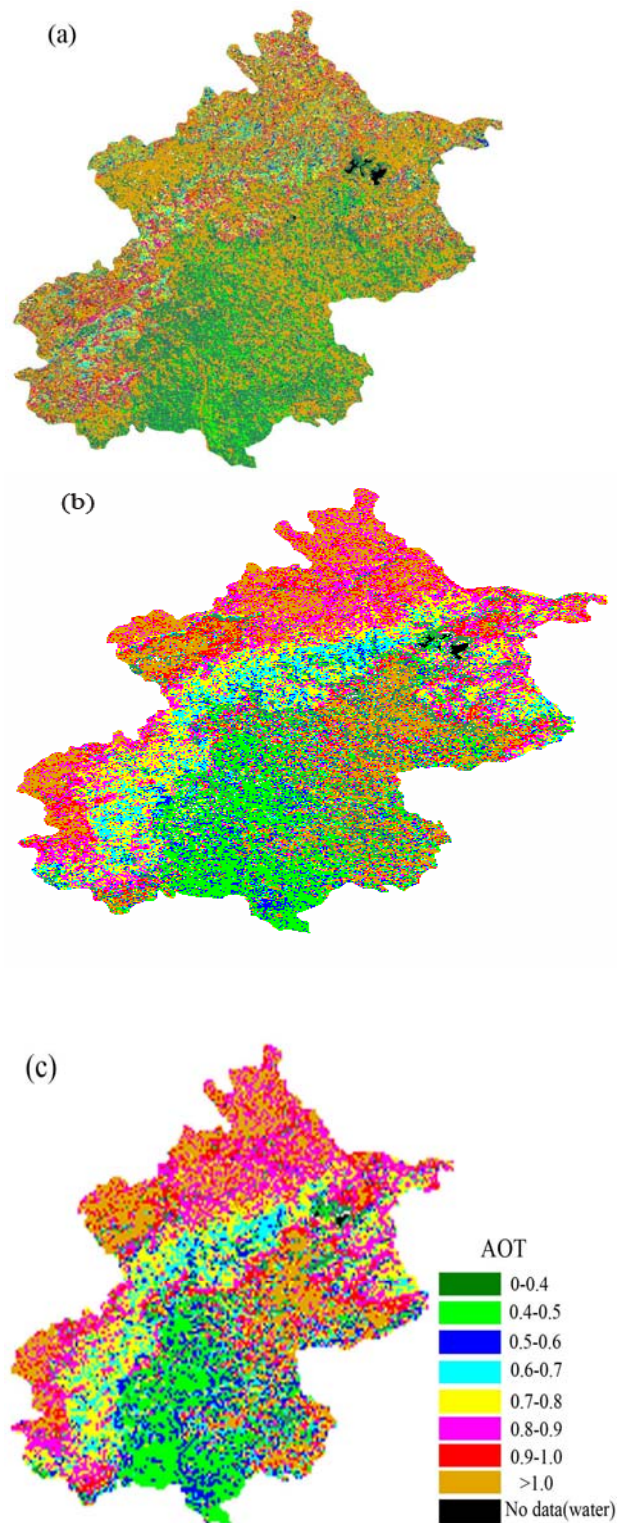


Figure 5. Retrieved AOT from Terra/MODIS band 4 (0.55 μ m) of (a) 250m resolution, (b) 500m resolution, (c) 1km resolution

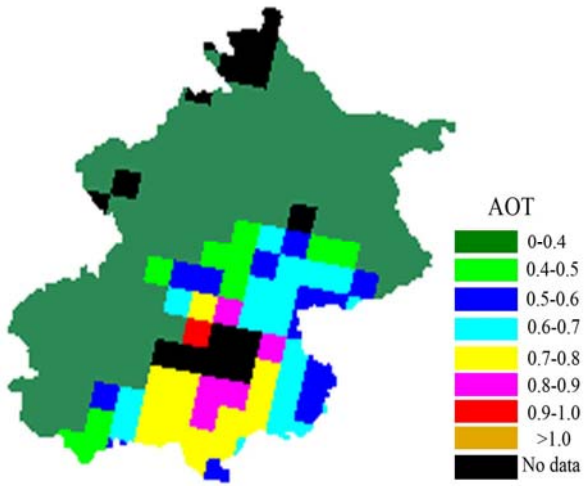


Figure 6. AOT at $\lambda=0.55\mu\text{m}$ from MOD04_L2